APPLIED ORGANOMETALLIC CHEMISTRY
Appl. Organometal. Chem. 2004; **18**: 1–8
Bioorganometallic Chemistry AOC
Published online in Wiley InterScience (www.interscience.wiley.com). DOI:10.1002/aoc.566

^{111}In–L–LDL and ^{153}Gd–L–LDL as radiotracers for detection of AR4-2J rat pancreatic tumors

Ginette Ratovo[1,2], Jean-Pierre Souchard[3], Pascale Urizzi[3], Yvon Coulais[4], Françoise Nepveu[3] and Etienne Hollande[1]*

[1]Laboratoire de Biologie Cellulaire et Moléculaire des Epithéliums EA3032, 38, Rue des 36 Ponts, Université Paul Sabatier, 31400 Toulouse, France
[2]INSERM U 531 Biologie et Pathologie Digestive, IFR31 CHU Rangueil, 1, Avenue J. Poulhès, 31403 Toulouse Cédex 4, France
[3]Laboratoire Pharmacochimie des Substances Naturelles et Pharmacophores Redox (UMR U152), 35, Ch des Maraîchers, Université Paul Sabatier, 31062 Toulouse, France
[4]Laboratoire Traceurs et Traitement de l'image EA 3033, 133, Route de Narbonne, Université Paul Sabatier, Toulouse, France

Pancreatic cancer has an extremely poor prognosis, due, in part, to lack of methods for early diagnosis. The present study was designed to evaluate the potential of labeling low-density lipoprotein (LDL) with a radionuclide using a lipid chelating agent, bis(stearylamide) of diethylenetriaminepentaacetic acid (L), to detect pancreatic tumors by gamma-scintigraphy. Previous studies indicated that the difficulty of visualization of pancreatic tumors was due to their poor vascularization. This study compares the ability of two radiotracers, ^{111}In–L–LDL and ^{153}Gd–L–LDL to target highly vascularized rat pancreatic tumors (AR4-2J) implanted in nude mice. Biodistribution studies showed that the tumor uptake of ^{111}In–L–LDL and ^{153}Gd–L–LDL tracers was twofold and fivefold higher respectively than with the controls (^{111}In citrate and ^{153}Gd citrate respectively). These tracers would thus be suitable for scintigraphic imaging.

We show here that LDL could be employed as a delivery system for tracers such as ^{111}In or ^{153}Gd when these two radionuclides are complexed by a lipid-chelating anchor, and that ^{111}In–L–LDL and ^{153}Gd–L–LDL enabled better visualization of the pancreatic tumor tissues, with a better result with ^{153}Gd–L–LDL.

KEYWORDS: exocrine pancreatic tumor; indium-111; gadolinium-153; low-density lipoprotein labeling; radiotracer; tumor targeting; scintigraphic images; AR4-2J cell line

INTRODUCTION

Pancreatic cancer has the fourth highest mortality rate for cancer in men and the fifth highest in women. The 5 year survival is 3 to 8%.[1] This poor prognosis is due to the lack of methods for early diagnosis, the aggressive nature of pancreatic adenocarcinomas and their resistance to antineoplasic drugs. Early diagnosis would help treatment by surgical excision, and thus reduce the mortality rate. Various methods have been investigated for early detection of pancreatic tumors. However, suitable conditions for specific targeting of drugs or markers to pancreatic tumor cells have yet to be established. Monoclonal antibodies have been employed as natural vectors of diagnostic or cytotoxic agents to target primary human cancers and their metastases.[2–7] Low-density lipoproteins (LDLs) have been proposed,[8–13] as cancer cells express more LDL receptors (R–LDL)[14,15] than do healthy cells apart from hepatocytes.[16] The internalization and intracellular degradation of LDLs mediated by their specific receptors has favored the use of such particles as vectors of therapeutic or diagnostic agents to various types of tumor, especially pancreatic tumors.[17] A recent study on pancreatic adenocarcinomas, however, gave disappointing results.[18] We found that LDL labeled with radioactive indium did not readily reach pancreatic xenografts produced by inoculation of nude mice with cancerous human pancreatic duct cells of the Capan-1 line, whereas, *in vitro*, such particles

*Correspondence to: Etienne Hollande, Laboratoire de Biologie Cellulaire et Moléculaire des Epithéliums, 38, Rue des 36 Ponts, Université Paul Sabatier, 31400 Toulouse, France.
E-mail: hollande@lmtg.ups-tlse.fr
Contract/grant sponsor: Ministry of National Education, Research and Technology.
Contract/grant sponsor: Conseil Régional Midi-Pyrénées, France.

bound to the surface of cells and were internalized by them.[17] This was accounted for by weak angiogenesis after heterotransplantation into nude mice of Capan-1 cells in contrast to the strong angiogenesis observed in xenografts of human melanoma cells.[18]

Here, we present results in favor of this hypothesis using cancerous pancreatic cells of the AR4-2J line heterotransplanted into nude mice. These xenografts of rat origin are strongly vascularized in this host. The low level of Capan-1 cell radiolabeling was thought to be due to the relatively poor internalization of this radioelement by these cells. We thus compared indium with other radiometals for their ability to target tumors. In this study, gadolinium was selected because gadolinium-based compounds are used as contrast agents in magnetic resonance imaging (MRI). Gadolinium has also been proposed as an alternative to boron for neutron capture therapy of tumors ($^{157}Gd/^{10}B$). The success of all these diagnostic and therapeutic strategies is dependent on the localization and retention of high concentrations of the selected metal within the target tumor.

We compared two radiometals, ^{111}In and ^{153}Gd, in targeting pancreatic AR4-2J xenografts in mice using LDL as vector and diethylenetriaminepentaacetic acid (DTPA)-bis(stearylamide) (L) as chelating agent. Although both radiotracers visualized the tumor, ^{153}Gd had superior sensitivity.

MATERIALS AND METHODS

AR4-2J cell culture

AR4-2J cells were grown in Dulbecco's modified Eagle's medium (DMEM; GIBCO, Grand Island, New York, USA) supplemented with 4.5 g l^{-1} of glucose and 10% fetal calf serum (Life Technologies, Inc., Eragny, France). The cells were seeded at 100 000 cells ml^{-1} into 25 cm^3 plastic flasks. They were maintained by successive passages after trypsinization (0.05% Trypsin, 0.02% elthylenediaminetetraacetic acid, Life Technologies, Inc., Eragny, France). Medium was renewed every 2 days. The cultures were checked regularly for the absence of contamination by mycoplasma using cultures grown in a suitable medium for three passages and polymerase chain reaction methods (Mycoplasma PCR kits, Stratagene, CA).

AR4-2J xenografts

All animal experiments were carried out in conformity with the Declaration of Helsinki and the 'Guiding Principles in the Care and Use of Animals' approved in its revised form by the American Physiological Society, 1991. AR4-2J xenografts were obtained by subcutaneous injection.[19] Briefly, 4×10^6 3-day-old AR4 2J cells in culture between the 19th and the 46th passages were injected into the dorsal region or the right hind leg of 4–6-week-old congenitally athymic nu/nu female mice (Iffa Credo, Lyon, France) maintained in a pathogen-free environment. Tumor growth was followed for 30 days by measuring tumor volumes in two groups of six mice. The length l, width w and height h of each tumor were measured with a slide caliper. The volume was calculated from the ellipsoid volume:

$$V = \frac{4}{3}\pi\frac{lwh}{2}$$

Cytology

In order to define the structure, the degree of vascularization and the growth of the xenografts, samples of tumor aged 7, 14, 17 and 30 days used for scintigraphic imaging were removed. They were fixed in Bouin's solution, dehydrated and embedded in paraffin. The sections of tumor were stained with hemalum–eosin and Mallory's trichrome.

Preparation of the ligand, DTPA-bis(stearylamide) (L)

L was prepared as previously reported:[20] stearylamine (0.539 g; 2 mmol) in 40 ml of chloroform at 40 °C was added slowly to a solution of DTPA bisanhydride (0.393 g; 1.1 mmol) in 50 ml of dimethylformamide (DMF). After 2 h under stirring at 40 °C, the colorless solution was cooled at 4 °C for 2 h. The white precipitate was collected by filtration, washed with acetone (3 × 100 ml), and dried at 80 °C overnight. The precipitate was crystallized in boiling ethanol (800 ml). After 24 h at room temperature, the small crystals were collected by filtration and washed with water (800 ml, 80 °C, 3 h) and with chloroform (800 ml, reflux, 3 h) to eliminate unreacted DTPA and stearylamine. L was obtained in 45% yield. Purity of the product was checked by thin-layer chromatography (TLC; chloroform/methanol/water/acetic acid, 50 : 30 : 8 : 4, v/v; $R_f = 0.37$). Covalent linkage of the two stearyl chains per DTPA molecule and symmetry of the ligand were shown by ^1H, ^{13}C, and ^1H–^1H COSY NMR studies.

Preparation of LDLs and the conjugates, L–LDL

Human LDLs ($d = 1.019$–1.050 g ml^{-1}) were isolated from fresh human plasma of healthy volunteers by KBr gradient ultracentrifugation (197 000 g, $10 < t < 15$ °C) and KBr for density adjustment. After storage at 4 °C and before experimentation, LDL samples were filtered and protein concentration was determined using BSA as standard.[21,22] For simplicity, milligrams per millilitre instead of milligrams of protein per millilitre will be used as the unit of LDL concentration in the text. Solutions of L were prepared from aqueous ammonia solution (NH_4OH–NH_4Cl, pH 9–9.5, 0.15 M) with vigorous stirring at 50 °C. The concentrations of L were determined by an indirect spectrophotometric method using excess of zinc(II) sulfate. The L–LDL particles were prepared by adding dropwise 190 µl and of the diluted L solution (1.5 mM) to a solution of LDL (1.7 mg ml^{-1}) for experiments carried out with ^{111}In. The L–LDL particles were prepared by adding dropwise 218 µl of the diluted L solution (1.5 mM) to a solution of LDL (2 mg ml^{-1}) for experiments carried out with ^{153}Gd. These preparations were stirred for 1 h and filtered. The volume of the added solution of L was

always approximately 50 times lower than the volume of the LDL solution to maintain pH 7.4.

Preparation of ^{111}In–or ^{153}Gd–L–LDL radiotracers

The carrier-free $^{111}InCl_3$ and $^{153}GdCl_3$ (gamma-emitters) were obtained from NEN Research Products (USA). For the preparation of ^{111}In–L–LDL particles, $InCl_3$ (1.13×10^{-6} M in 0.05 M HCl) was added to $^{111}InCl_3$ (74 MBq, 2.0 mCi, 152 Ci mg^{-1} indium atoms in 0.05 M HCl) to produce a final solution of 50 µl. Sodium citrate solution (200 µl, 2.73×10^{-6} M) and 2%NH_4OH(3 µl) were added to produce the final solution at pH 7.4. Sodium citrate was used to avoid the formation of metallic hydroxides. This solution was added to L–LDL samples with an appropriate volume to obtain a 3/100 In–L/LDL ratio (In-to-L ratio, 1:1), stirred 1 h and filtered to remove free and insoluble In–L complexes. For the preparation of ^{153}Gd–L–LDL particles, $^{153}GdCl_3$ solution (3.7 MBq, 100 µCi, 5 Ci g^{-1} gadolinium atoms in 0.5 M HCl, 100 µl, 1.27 mM) was added to sodium citrate solution (400 µl, 1.58 mM). 2%NH_4OH(3 µl) was added to produce the final solution at pH 7.4. This solution was added to L–LDL samples with an appropriate volume to produce a 30/100 Gd–L/LDL ratio (Gd-to-L ratio, 1:1), stirred for 1 h and filtered to remove free and insoluble Gd–L complexes. The formulae of the ^{111}In–L–LDL and ^{153}Gd–L–LDL radiotracers are schematized in Fig. 1.

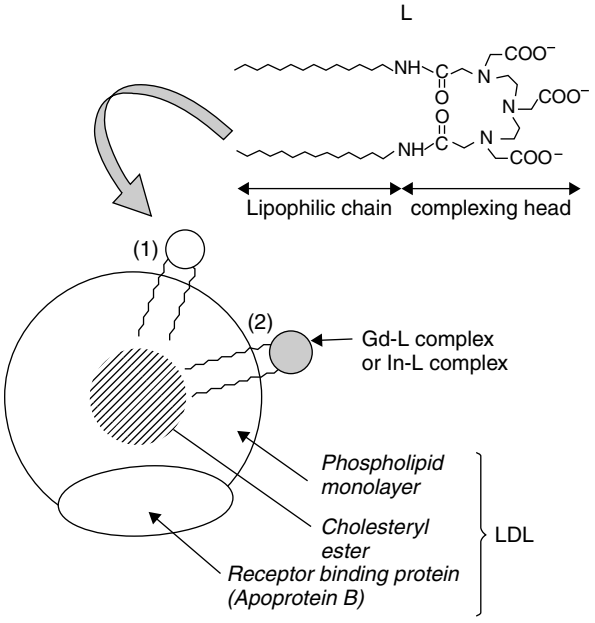

Figure 1. Schematic presentation of the Gd–L–LDL and In–L–LDL particles. The complexing ligand L was first incorporated into the LDL monolayer (1), and then gadolinium or indium was chelated by L (2).

Scintigraphy

$^{111}InCl_3$, ^{111}In–L–LDL, $^{153}GdCl_3$, ^{153}Gd–L–LDL, were injected intravenously to give 9.3 MBq (250 µCi) for ^{111}In and 0.93 MBq (25 µCi) for ^{153}Gd per mouse. The radiotracer was injected when the tumors reached a volume of 360 mm^3, i.e. about 17 days after inoculation. Mice were anesthetized before experimentation with a sterile solution of immenoctal (Houdé, Paris, France; 300 µl intraperitoneal per mouse). The animals were subjected to scintigraphic imaging ($n = 6$ mice) 4, 24, 48 and 72 h after injection, using a gamma camera (Sophycamera) equipped with a pinhole collimator 70 mm away from the animal. Animals were sacrificed 72 h after injection (half-life of LDL) and tissues samples were set apart (tumor, stomach, intestine, pancreas, muscle), blotted dry, weighed and counted for radioactivity in a gamma counter (Packard Auto Gamma 5780). The results were expressed as percentage of injected dose per gram of tissue (%ID g^{-1} of tissue) plus/minus standard deviation (SD) for the different organs.

RESULTS

In order to determine the most favorable stage for the scintigraphic analysis, the growth and the structure of the xenografts were examined at different ages. We obtained a 100% 'take' rate at all inoculation sites ($n = 12$), with tumors appearing between 4 and 6 days after inoculation. In this period, the rate of growth was slow, subsequently increasing rapidly with a doubling time of 2 days (Fig. 2).

The tumor reached a volume of 360 mm^3 by day 17. Beyond this stage, the highly vascularized tumors became hemorrhagic. The tumors adherent to the internal side of the skin were surrounded by numerous blood vessels. Certain peritumoral vessels attained a diameter of 100 µm. Figure 3a

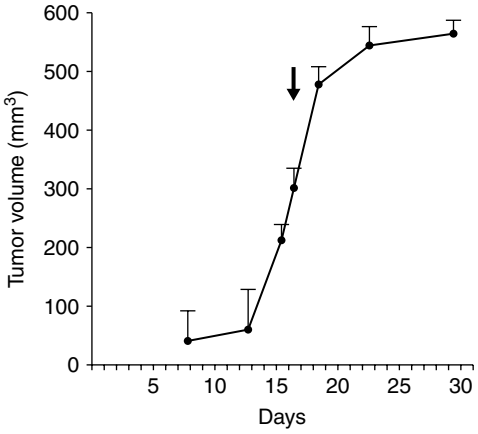

Figure 2. Growth curve of AR4-2J xenografts over 30 days. The arrow indicates the stage selected for the scintigraphic imaging. Results are means plus/minus standard error of the mean; $n = 12$.

illustrates the extent of the vascularization in the AR4-2J xenografts. Microscopic examination of the tumor highlighted numerous small vessels in the tumoral stroma of 9-day-old xenografts (Fig. 3b, arrows). They were dispersed in a tumoral tissue consisting of an association of numerous small cells in tumor nodules (Fig. 3b). The reactive connective tissue

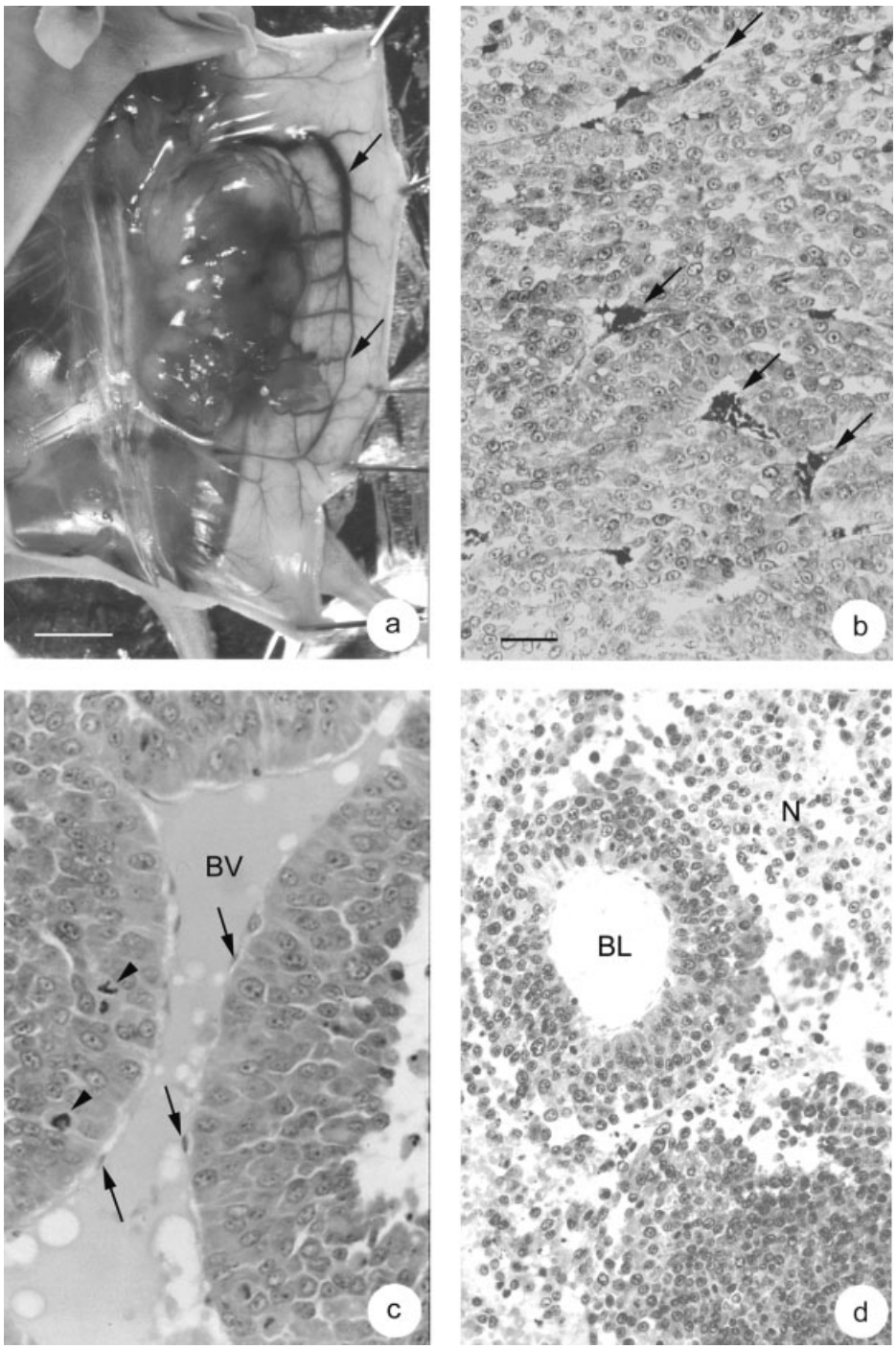

Figure 3. (a) Macroscopic appearance of a 17-day-old AR4-2J xenograft. Note the bulk of the tumor and the extensive vascularization (arrows). Bar: 0.65 cm. (b) Histological section of a tumoral nodule of 14-day-old AR4-2J xenograft showing the numerous intratumoral blood capillaries (arrows). Note the absence of reactive connective tissue. Bar: 50 μm. (c) 19-day-old AR4-2J xenograft. Histological section exhibiting the marked dilatation of blood vessels (BV). The arrows indicate the vascular endothelium. The arrow heads show mitosis in the cells lining the capillaries. Bar: 20 μm. (d) Appearance of 30-day-old xenograft. Note the wide areas of necrosis (N) and the coronal organization of cancerous cells around the blood lacuna (BL). Bar: 50 μm. Hemalum–eosin staining.

was poorly developed. In the older xenografts (17 days old), we noted marked dilatation of the blood vessels (Fig. 3c). At this stage, certain cancerous cells were in mitosis and the tumor joined with the walls of vessels (Fig. 3c, arrows). The AR4-2J tumors removed after the 17th day appeared spongiform and were markedly hemorrhagic. Histological examination revealed intense necrosis in the middle of the tumor nodules and many blood lacunas (Fig. 3d). These gaps were large and only partially surrounded by endothelium. The cancerous cells, some of which were in mitosis, were in direct contact with the blood (Fig. 3c). Xenograft growth was identical in all inoculation sites. For the scintigraphic imaging of tumors after intravenous inoculation of ^{111}In and ^{153}Gd, therefore, we employed the 17-day-old xenografts with healthy vascularization.

Scintigraphic tumor imaging and *in vivo* biodistribution of ^{111}In and ^{153}Gd radiotracers

Scintigraphic imaging in the nude mouse transplanted with pancreatic AR4-2J cells (Fig. 4) clearly visualized the tumor

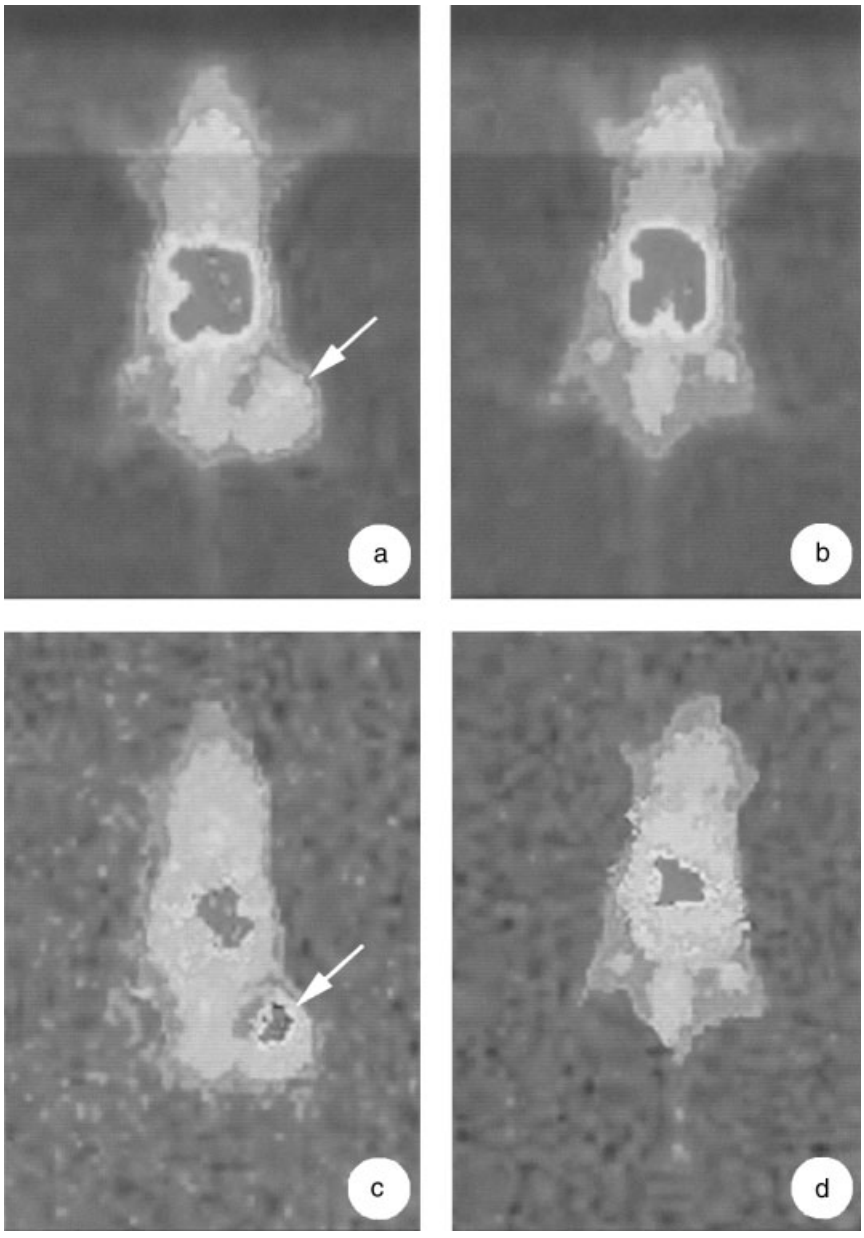

Figure 4. Gamma-camera images of nude mice xenografted with rat pancreatic tumor (AR4-2J) showing the distribution of radiotracers ^{111}In–L–LDL (a) or ^{153}Gd–L–LDL (c). Note the weak uptake of radioactivity in the tumors after injection of ^{111}In citrate (b) or ^{153}Gd citrate (d). The images were taken 72 h after intravenous injection of the tracer. Note the strong radioactivity of xenografted AR4-2J after injection of ^{153}Gd–L–LDL (c, arrow).

in the right hind leg of each animal after injection of the ^{111}In–L–LDL (Fig. 4a, arrow) or ^{153}Gd–L–LDL radiotracer (Fig. 4c, arrow). No tumors were detectable after injection of ^{111}In citrate (Fig. 4b) or ^{153}Gd citrate (Fig. 4d; control). This result showed that the radiometals bound to LDL were specifically transported toward the tumor by LDL. It is noteworthy that the contrast of the tumor was better with the ^{153}Gd–L–LDL (Fig. 4c, arrow).

The radioactivity could be followed *in vitro* in real time by scintigraphic imaging with a gamma camera. The observed radioactivity in the tumors reached a plateau after 24 h (Fig. 4). The radioactivity count in the tumor after injection of the ^{111}In–L–LDL particles (0.108 ± 0.016 tumor counts/mouse counts) was double that after injection of ^{111}In citrate complex (0.055 ± 0.008 tumor counts/mouse counts) (Fig. 5a). Likewise, the radioactivity in the tumors was six-fold higher using ^{153}Gd–L–LDL particles (0.107 ± 0.0045 cpm tumor/cpm total mouse) instead of ^{153}Gd citrate (0.020 ± 0.0025 cpm tumor/cpm total mouse) (Fig. 5b).

In vivo biodistribution in tumor-bearing mice on the third day

The uptake of ^{111}In citrate, ^{111}In–L–LDL, ^{153}Gd citrate and ^{153}Gd–L–LDL radioactivity by the tissues is illustrated in Figure 5. A low level of radioactivity was observed in stomach, intestine, pancreas, muscle and blood.

Considerably more radioactivity was observed in the tumor after injection of ^{111}In–L–LDL than after ^{111}In citrate, (2.5 ± 0.22%ID g^{-1} versus 1.02 ± 0.12%ID g^{-1}) (Fig. 6).

Similarly, more radioactivity was observed in the tumor after injection of ^{153}Gd–L–LDL than after ^{153}Gd citrate (3.9 ± 0.11%ID g^{-1} versus 0.75 ± 0.16%ID g^{-1}) (Fig. 7).

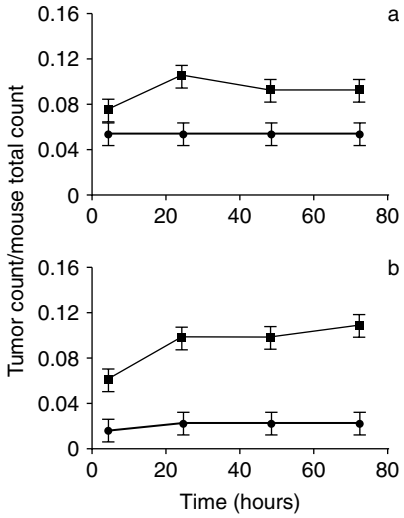

Figure 5. Uptake of radioactivity on gamma-scintigraphic images: (a) radioactive uptake 4, 24, 48 and 72 h after intravenous injection of ^{111}In–L–LDL (■) or ^{111}In citrate (♦) into AR4-2J pancreatic tumor-bearing mice; (b) radioactive uptake 4, 24, 48 and 72 h after intravenous injection of ^{153}Gd–L–LDL (■) or ^{153}Gd citrate (♦) into AR4-2J pancreatic tumor-bearing mice. Note the same levels of radioactivity after injection of 3/100 In–L/LDL (a) and 30/100 Gd–L/LDL (b). The results are expressed as the ratio of tumor counts to total mouse counts plus/minus standard deviation.

The high level of radioactivity of the tumoral tissue after intravenous injection of ^{111}In–L–LDL and ^{153}Gd–L–LDL was

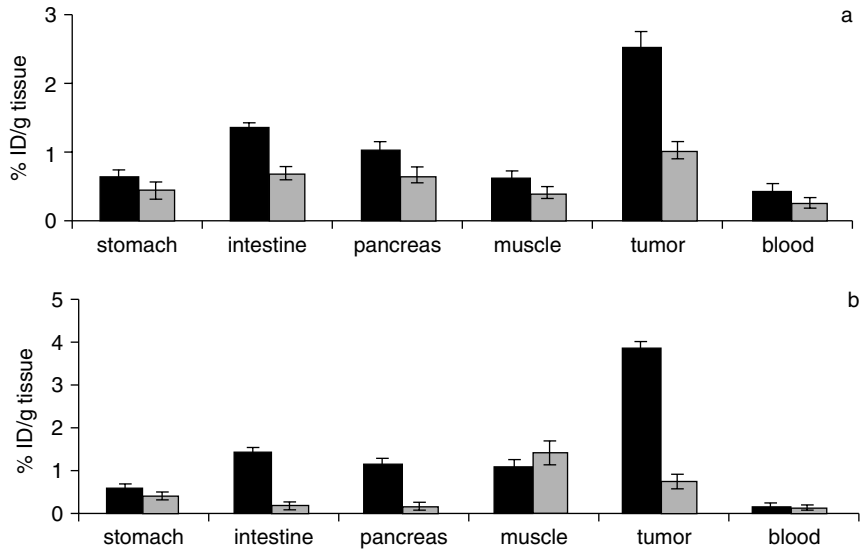

Figure 6. Comparative biodistribution of radiolabeled ^{111}In–L–LDL (■) or ^{111}In (▨) (a) and radiolabeled ^{153}Gd–L–LDL (■) or ^{153}Gd (▨) (b) in AR4-2J pancreatic xenografts and different organs, 72 h after intravenous injection. Note the strong radioactivity in the tumors with respect to that in other organs and the extent of radioactivity of the tumors compared with controls. The results are expressed as the ratio percent injected dose (ID) per gram organ plus/minus standard deviation.

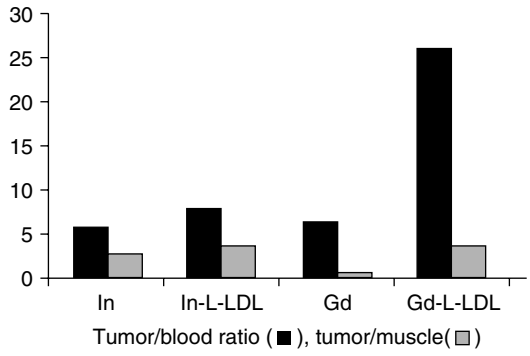

Figure 7. Biodistribution of ^{111}In, ^{111}In–L–LDL, ^{153}Gd and ^{153}Gd–L–LDL tracers, in tumor and muscles given as the ratios tumor/blood (■), tumor/muscle (▨), 72 h after intravenous injection. Note: (i) the higher level of radioactivity in tumor obtained with the ^{153}Gd–L–LDL than with ^{111}In–L–LDL; (ii) the stronger radioactivity in tumor than in muscles.

shown by the tumor/blood or tumor/muscle ratios. The tumor/blood ratio was 3.2-fold higher with ^{153}Gd–L–LDL than with ^{111}In–L–LDL.

DISCUSSION

The results presented here show that LDL vectors labeled with ^{111}In or ^{153}Gd enabled visualization by gamma scintigraphy of pancreatic rat tumors (AR4-2J) heterotransplanted into nude mice. In a previous study, we suggested that the ability of ^{111}In–L–LDL tracers to detect human pancreatic tumors by scintigraphy depended on the degree of vascularization of the tumor.[18] To support this interpretation, we investigated strongly vascularized pancreatic xenografts. Various cancerous human pancreatic lineages maintained *in vitro* have been heterotransplanted into nude mice to determine the extent of angiogenesis. Cells of the MIA-PACA-2,[23] BxPC-3,[24] PANC-1,[25] CFPAC-1,[26] and CFPAC-PLJ-CFTR6[27] lines heterotransplanted into the nude mouse produced poorly vascularized tumors. Scintigraphic images with poor contrast were obtained after injection of ^{111}In–L–LDL to mice bearing such xenografts (data not shown). On the other hand, cells of the AR4-2J line heterotransplanted into nude mice produced tumors with a 100% 'take'. The AR4-2J xenografts grew rapidly. After 7 days, the tumoral nodules were seen to be irrigated with numerous blood vessels. In older tumors, the vessels became highly dilated. In later stages, proliferating cancer cells were in direct contact with the blood after rupture of vessel walls. At this stage of growth, the blood-filled AR4-2J xenografts had a spongiform appearance. The presence of numerous intratumoral capillaries in the early stages of growth prompted us to test LDLs as vectors of radioactive elements for scintigraphic visualization of the pancreatic xenografts. The gamma-scintigraphic images of xenografted nude mice made 72 h after injection of the ^{111}In–L–LDL radiotracers clearly showed the AR4-2J pancreatic tumor in the right hind limb. We did not inject cells into dorsal regions to avoid confusion of images of pancreatic tumors with those of the liver, an organ that strongly expresses LDL receptors.[16] The poor AR4-2J tumor images obtained after intravenous injection of the radiometal alone (^{111}In citrate) compared with the quality of images obtained after injection of the radiotracers (^{111}In–L–LDL) pointed to a specific targeting of the tumors via LDL receptors. The tenfold higher levels of LDL receptors in pancreatic cancerous cells, the demonstration of the binding and the internalization of LDL bearing radioactive indium in the cytoplasm of cancerous pancreatic cells, and in perinuclear regions of the cytoplasm,[17] argue in favor of the targeting of the radiotracers via the R–LDL. Two radiotracers were chosen, the first labeled with ^{111}In and the second with ^{153}Gd. In both cases, a chelating agent, DTPA-bis(stearylamide), was used to stabilize the radiometal on the surface of LDL after anchorage of the ligand in the phospholipid monolayer. The high stability constant of the In–L complex and the presence of an eight-coordinated In^{3+} single structural isomer in aqueous solution were deduced by comparison with the results obtained from potentiometric and NMR studies for the DTPA-bis(butanamide) derivative (DTPA-$(BuA)_2$), which was used as a model for reasons of solubility.[28] The two complexes In–L and Gd–L have neutral charge and are insoluble in aqueous buffered solutions at pH 7.4 and have high lipophilicity and solubility in lipid phases, e.g. LDL.[29] Previous *in vitro* experiments[20] had demonstrated the stability of the lipophilic anchorage of the ligand L and the stability of the metal complexation on the L–LDL conjugates in plasma.

The strong intratumoral radioactivity observed after injection of ^{153}Gd–L–LDL and the well-contrasted scintigraphic images pointed to a superior targeting of this complex in the tumor.

Analysis of the biodistribution 72 h after intravenous injection showed strong uptake in the liver for both radiotracers, suggesting that the indium and gadolinium were transported by LDL to the liver, an organ that is known to express LDL receptors.[16] The biodistribution analysis showed a twofold higher level of radioactivity in the AR4-2J tumor after injection of the ^{111}In–L–LDL radiotracer and fivefold more after injection of the ^{153}Gd–L–LDL radiotracer than after injection of control compounds (metal citrate) containing identical amounts of ^{111}In or ^{153}Gd. These results confirm those from direct counting of the radioactivity on the scintigraphic images. In all the experiments, we also noted a higher level of radioactivity in the AR4-2J pancreatic tumors than in all other organs except the liver. As this tumor was highly vascularized, the high level of radioactivity in the tumor could be accounted for by its high blood content. However, the weak radioactivity observed in blood strongly suggests that the high level of radioactivity in the tumor was due to a significant ^{111}In–L–LDL or ^{153}Gd–L–LDL uptake by the cells. These observations indicated that either of these radiotracers could be exploited for detection of cancers of the pancreas in other

animal models where pancreatic tumors either are induced or occur spontaneously. The LDLs specifically vectorize indium or gadolinium to the pancreatic tumor AR4-2J, although we found that uptake was superior with the gadolinium complex.

Gamma camera studies confirmed the retention of the radiotracers in the tumor. Contrary to the hydrophilic Gd(DTPA) derivatives used as extracellular MRI agents,[30] the ^{153}Gd–L–LDL conjugate used in the present experiments was highly lipophilic. The stability of the gadolinium chelates *in vivo*, their high lipophilicity and the R–LDL pathway could explain the better result observed with the ^{153}Gd–L–LDL tracer.

In conclusion, ^{111}In–L–LDL and ^{153}Gd–L–LDL may be useful radiotracers for localization of pancreatic tumors. Uptake appeared to be more selective with the gadolinium than with the indium complex.

Acknowledgments

This work was supported by the Ministry of National Education, Research and Technology (MENRT) and the Conseil Régional Midi-Pyrénées, France.

REFERENCES

1. Janes Jr RH, Niederhuber JE, Chmiel JS, Winchester DP, Ocwieja KC, Karnell JH, Clive RE, Menck HR. *Ann. Surg.* 1996; **223**: 261.
2. Takahashi H, Adachi K, Yamaguchi F, Teramoto A. *Anticancer Res.* 1999; **19**: 4151.
3. Weiner LM. *Semin. Oncol.* 1999; **26**: 41.
4. Monneret C, Florent JC. *Bull. Cancer* 2000; **87**: 829.
5. Milenic DE. *Curr. Pharm. Des.* 2002; **8**: 1749.
6. Ross J, Gray K, Schenkein D, Greene B, Gray GS, Shulok J, Worland PJ, Celniker A, Rolfe M. *Expert Rev. Anticancer Ther.* 2003; **3**: 107.
7. Trail PA, King HD, Dubowchik GM. *Cancer Immunol. Immunother.* 2003; **52**: 328.
8. Hynds SA, Welsh J, Stewart JM, Jack A, Soukop M, Mcardle CS, Calman KC, Packard CJ, Sheperd J. *Biochem Biophys. Acta* 1984; **4**: 795.
9. Lundberg B. *Cancer Res.* 1987; **47**: 4105.
10. Vitols S. *Cancer Cell.* 1991; **3**: 488.
11. Dubowchik GM, Firestone RA. *Bioconjug. Chem.* 1995; **6**: 427.
12. Koller-Lucae SK, Schott H, Schwendener RA. *Br. J. Cancer* 1999; **80**: 1542.
13. Kader A, Pater A. *J. Control. Release* 2002; **80**: 29.
14. Vitols S, Peterson C, Larsson O, Holm P, Aberg B. *Cancer Res.* 1992; **52**: 6244.
15. Maletinska L, Blakely EA, Bjornstad KA, Deen DF, Knoff LJ, Forte TM. *Cancer Res.* 2000; **60**: 2300.
16. Rudling MJ, Reihner E, Einarsson K, Ewerth S, Angelin B. *Proc. Natl. Acad. Sci. U.S.A.* 1990; **87**: 3469.
17. Urizzi P, Souchard JP, Palévody C, Ratovo G, Hollande E, Nepveu F. *Int. J. Cancer* 1997; **70**: 315.
18. Urizzi P, Souchard J-P, Ratovo G, Coulais Y, Nepveu F, Hollande E. *Appl. Organometal. Chem.* 2003; **17**: 212.
19. Estival A, Louvel D, Couderc B, Prats H, Hollande E, Vaysse N, Clémente F. *Cancer Res.* 1993; **53**: 1182.
20. Jasanada F, Nepveu F. *Tetrahedron Lett.* 1992; **33**: 5745.
21. Jasanada F, Urizzi P, Souchard JP, Le Gaillard F, Favre G, Nepveu F. *Bioconj. Chem.* 1996; **7**: 72.
22. Jasanada F, Urizzi P, Souchard JP, Favre G, Boneu A, Nepveu F. *J. Chem. Phys.* 1996; **93**: 128.
23. Yunnis AA, Arimura GK, Russin DJ. *Int. J. Cancer* 1977; **19**: 218.
24. Tan MH, Nowak NJ, Loor R, Ochi H, Sandberg AA, Lopez C, Pickr JW, Berian R, Douglass Jr HO, Chu TM. *Cancer Invest.* 1986; **4**: 15.
25. Lieber M, Mazzetta J, Nelson-Rees W, Kaplan M, Todaro G. *Int. J. Cancer* 1975; **15**: 741.
26. Schoumacher RA, Ram J, Iannuzzi MC, Bradbury NA, Wallace RW, Hon CT, Kelly DR, Schmid SM, Gelder FB, Rado TA, Frizzell RA. *Proc Natl Acad. Sci. U. S. A.* 1990; **87**: 4012.
27. Drumm ML, Pope HA, Cliff WH, Rommens JM, Marvin SA, Tsui LC, Collins FS, Frizzell RA, Wilson JM. *Cell* 1990; **62**: 1227.
28. Geraldes CFGC, Delgado R, Urbano AM, Costa J, Jasanada F, Nepveu F. *J. Chem. Soc. Dalton Trans.* 1995; 327.
29. Urizzi P, Souchard JP, Tafani JAM, Coulais Y, Nepveu F. *J. Chem. Phys.* 1997; **94**: 371.
30. Caravan P, Ellison JJ, McMurry TJ, Lauffer RB. *Chem. Rev.* 1999; **99**: 2293.

